commitment continues advancing toward both sides of the cell mass.

The expression of Sox9 and the synthesis of collagen type II and GAGs also indicated spontaneous chondrogenesis during this morphogenic development (**Figure 7 C, D** and **Figure 9 C–E**). Sox9, Runx2, and collagen type II, like brachyury, showed a profile of expression strongly related to morphogenic development, although it remains unknown how the morphological changes proceeded as function of the expression of these genes. Loss-of-function experiments would elucidate the exact relationship between gene expression and the morphogenic process. Sox9 was strongly over-expressed at two time-points during the morphogenetic event related to physical changes: strong isotropic contraction (stage 2) and closure of the 3D bilaterality (stage 4).

Sox 5 and Sox6 were expected to follow the pattern of expression of Sox9, as their expression is dependent on the presence of Sox9 [65], but the results showed a different pattern. Sox5 was expressed in fibroblasts whether they were cultured in 2D, 3D with TGF-β or 3D without supplemented TGF-β, but in these latter conditions the expression of Sox5 was about 6.5 times higher based on the quantitative PCR results (**Figure 8**). More interesting is that Sox6 was only detected in MEFs cultured without TGF-β, which means that, assuming these culture conditions mimic stage 2 of the morphogenetic process, only MEFs in stage 2 of contraction have an active combination of the Sox trio (Sox9, Sox5 and Sox6) that is known to be key in the development of cartilage [66, 78-80]. As the Sox trio is expressed until chondrocytes become proliferating or hypertrophic [65], it is likely that at stage 4 of contraction MEFs have become either proliferating chondrocyte-like cells or cells with a similar phenotype to hypertrophic chondrocytes, although this should be confirmed with experimental data (**Figure 11**).

Altogether, the expression pattern of the Sox genes shows that Sox9 is required during two stages of the morphogenetic phenomenon: I) During contraction (Stage 2) and II) After closure of the structure (stage 4), while Sox5 and Sox6 are only significantly present in Stage 1-2. In his first peak of expression (**Figure 7 D**), Sox9 triggers the cell condensation that is taking place and prepares cells to undergo the morphogenic process, as happens in mesenchymal condensation during development. Then, Sox9 expression falls (**Figure 7 D**), which differs from the expression profile of Sox9 during chondrogenesis [62], but after that, a second peak of expression appears when the 3D structure is closed (**Figure 7 D**), just at the moment when mature cartilage would appear in a mesenchymal condensation process and Sox9 expression would reach its highest level in developmental chondrogenesis [62, 81]. In fact, after closure of the cellular structure, the expression of Sox9 is upregulated again and correlates with the synthesis of Collagen type II, meaning that, at this moment, chondrogenesis is taking place. Runx2 and Collagen type II expression levels are upregulated after closure of the structure and are maintained thereafter (**Figure 7 E**).

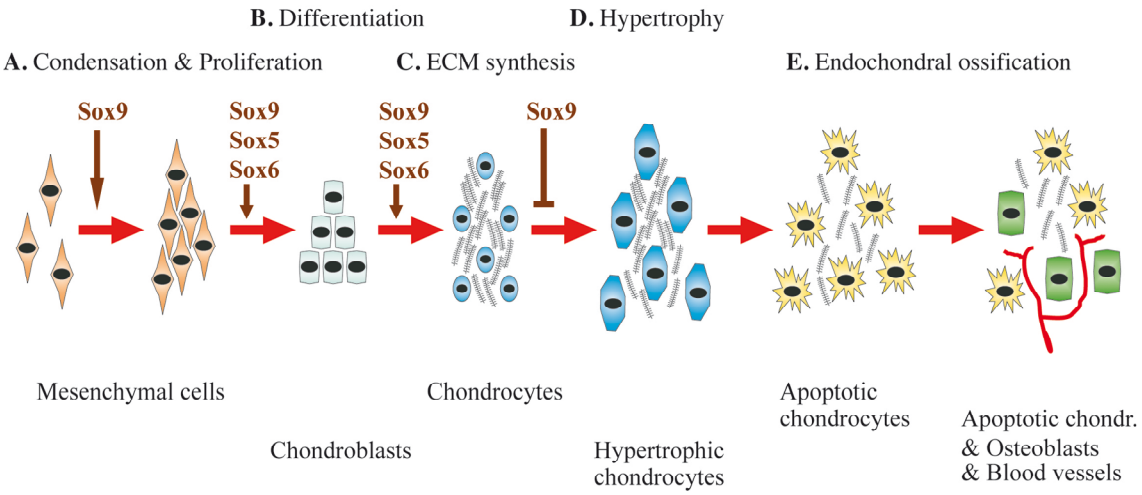

Figure 11: Schematic representation of the chondrogenesis and endochondral ossification.
(1) First mesenchymal cells condense to form a dense cell mass in a process that requires the expression of Sox9. (2) Mesenchymal cells proliferate and differentiate into chondroblasts. (3) These cells start secreting cartilage extracellular matrix (ECM) and become mature chondrocytes. Steps 2 and 3 of this process require the expression of the sox trio (Sox9, Sox6 and Sox5) (4) Eventually, chondrocytes grow to become hypertrophic and, if the tissue undergoes endochondral ossification, (5) cartilage is vascularized, ECM is degraded, hypertrophic chondrocytes become apoptotic and osteoblasts invade the free space within the tissue. Sox9 represses the chondrocytes' transition to hypertrophic chondrocytes thus inhibiting endochondral ossification.

Nevertheless, Sox5 and Sox6 are principally expressed at stage 2 of contraction and not in stage 4 (**Figure 8**). This may seem contradictory because Sox5 and Sox6 are downstream targets of Sox9 and should therefore follow the same pattern of expression, but when chondrocytes progress to hypertrophy Sox9 and Sox5 + Sox6 have opposite functions. Sox9 inhibits chondrocytes from entering hypertrophy while Sox5 and Sox6 enhance this progression [79]. Having different functions on hypertrophic chondrocytes might be accompanied by a different pattern of expression between the sox trio at this time point, although this comparison has not been analyzed yet. We also think that Sox5 and Sox6 need to be expressed in earlier stages of our morphogenetic process, although this remains to be proved. Many reasons support this hypothesis: first, Sox5 and Sox6 are required for the synthesis of aggrecan and collagen II [69, 78-80, 82] and then, Sox5 and Sox6 double-null mouse mutants develop chondrodysplasia, a disease characterized by the virtual lack of cartilage [65].

Link protein gene is transcribed simultaneously with aggrecan gene in the developing limb bud cartilage in chick [83] and human [84]. So we used the expression of link protein as a

gene reporter of the synthesis of proteoglycans. The results show that link protein is slightly expressed in MEFs at stage 2 of contraction and is not significantly expressed at stage 4 of contraction (**Figure 8**). This is surprising for one would expect to find a higher expression of link protein in samples of stage 4 of contraction, where there is an important increase in the production of glycosaminoglycans with respect to cells cultured in 2D (**Figure 7 C**). This contradiction can be explained by the fact that fibroblasts, even when cultured in 2D may have high levels of expression of link protein, as do monolayer cultured dedifferentiated chondrocytes –a cell type very similar to that of fibroblasts– after 6 passages [85]. Thus, a plausible parallelism can be established between the fibroblasts used for all our experiments and the well described dedifferentiated chondrocytes that form in monolayer *in vitro* cultures [86-90].

From the mechanical point of view, out of the experiments with different concentrations of RAD16-I (**Figure 2 B**) it seems clear that the biomechanics in early stages govern the process, at least in the first days of isotropic contraction where cells form a network and contract the system. It is very likely that, at early stages of this phenomenon, some genetic programs start taking control of the evolution of the system. At the time when the lateral contractions start to happen some genetic programs are already “ruling” the process. We are now focusing on early organizer genes to see if these are co-localized at the site and time when bilateral contractions take place.

Altogether we observed that the system undergoes organized contraction developing into a bilateral shape structure with a central axis, called 3D-bilateral structure, resembling an early vertebrate embryonic stage. These remarkable morphological changes suggest that the system might be engaging in a cellular self-organization process. We speculate that the initial conditions we provide to the cells (3D-culture of MEFs in self-assembling peptide scaffolds) recapitulates cellular and morphological changes of tissues undergoing development (proliferation, migration and condensation) and the expression pattern of early embryonic genes (organizers and tissue-specific genes) (**Figure 9 F**). Moreover, the process ends in the production of specific tissues such as patterned paraxial cartilage-like tissue. Most importantly, a group of differentiated cells under special “environmental conditions” can proceed to a self-organization process, characteristic of systems undergoing development.

In conclusion, the system we described here can be used to culture cells carrying specific mutations or transgenic genes and to obtain 3D-bilateral structures that recreate certain morphogenetic processes without the use of pregnant females and their embryos. We hope this model will contribute to the development of new paradigms within regenerative medicine. In future work, other cell sources such as dermal fibroblasts from amphibians and other mammals including adult humans will be tested to see if this particular self-organization phenomenon is common among other metazoans.

3.4. *Materials and Methods*

3.4.1. Culture of Mouse Embryonic Fibroblasts (MEF)

Mouse Embryonic Fibroblasts isolated from C57BL/6 embryos at day 14 were purchased from the American Type Culture Collection (scrc-1008; ATCC, Manassas, VA, USA). These fibroblasts (<9th passage) were cultured at 37ºC under 5% CO_2 in 75 or 175 cm^2 flasks. The medium used [fibroblast growth medium (FM)] contains DMEM high glucose with sodium piruvate (15-013-CV; Mediatech, Manassas, VA, USA) supplemented with 15 % (v/v) FBS (14-501F, Lonza, Allendale, NJ, USA), 4 mM L-glutamine (82007-322, VWR, West Chester, PA, USA), 100 µM MEM non essential amino acids (11140-050, Invitrogen, Carlsbad, CA, USA), 100 U/ml penicillin and 0.1 mg/ml streptomycin (20001, JR Scientific, Woodland, CA, USA).

Outside the USA, where the USA approved FBS produced by Lonza was not available, the fibroblast growth medium was supplemented with 20 nM of PDGF-BB (Recombinant Protein from rat, P4056 Sigma-Aldrich, St Louis, MO, USA). Cells were always maintained in a confluence percentage ranging from 45 % to 90 %.

3.4.2. Antibodies

Anti-digoxigenin sheep polyclonal antibody (11333089001) was purchased from Roche Diagnostics (Indianapolis, IN, USA). All other antibodies were purchased from Santa Cruz Biotechnology (Santa Cruz, CA, USA). Anti-Collagen type II (sc7764), anti-Brachyury (sc17743), anti-Nestin (sc21248) and anti-actin (sc1615) goat polyclonal antibodies and anti-PEBP2αA (sc10758; also known as anti-runx2) and anti-Sox9 rabbit polyclonal antibodies were used as primary antibodies. Anti-sheep (sc2473), anti-goat (sc2020) and anti-rabbit (sc2317) donkey antibodies HRP conjugated and FITC-labeled chicken anti-goat (sc2988) antibodies were used as secondary antibodies.

3.4.3. 3D Culture Technique

3.4.3.1. 3D-Culture technique with RAD16-I

MEFs (<9th passage) were trypsinized from the culture flasks, suspended in 20 % sucrose (S0389, Sigma-Aldrich, St Louis, MO, USA). Commercial 1 % RAD16-I (Puramatrix®, BD, Franklin Lakes, NJ, USA) was diluted with water to obtain a solution of 0.5 % RAD16-I. Then, equal volumes of the cell suspension in 20 % sucrose and RAD16-I (1 % or 0.5 %) were mixed to render a final cell suspension containing $2 \cdot 10^6$ MEFs/ml, 10 % sucrose and either 0.25 % or 0.5 % of RAD16-I. Alternatively, freshly isolated MEFs were suspended in 10 % sucrose and mixed with 0.5 % RAD16-I in 10 % sucrose, to obtain a final MEF concentration

of $2 \cdot 10^6$ cells/ml, 10 % sucrose and 0.20 – 0.25 % RAD16-I. This suspension (80 µl) containing cells and RAD16-I was loaded into 9 mm diameter cell culture inserts (PICM01250, Millipore, Billerica, MA, USA) previously placed inside 6-well culture plates (Nunc, Rochester, NY, USA). Then, 500 µl of Fibroblast Medium (FM) was added to the wells, outside the inserts. The medium penetrates the insert from the bottom membrane inducing a bottom to top self-assembly of RAD16-I, and thus, the formation of a gel with MEFs suspended inside the scaffold. After the gel was formed, 500 µl of FM was added on top of the hydrogel. The FM flows trough the gel washing out the remaining sucrose (**Figure 2 A**). This step was repeated two more times. Finally, 500 µl of FM were loaded inside the insert and 1.5 ml of FM in the well outside the insert. Incubation was performed at 37 ºC with 5 % CO_2 and medium was changed every 1-2 days. 3D cultures were maintained under these culture conditions typically during 7 to 15 days.

3.4.3.2. Fibroblast Media for the culture of MEFs in RAD16-I

The media used to culture MEFs in RAD16-I depend on the cellular response to the stimulus the media cause to the cells. In most of the experiments we looked for a tissue contraction in the cell culture so the composition of the media was adjusted to achieve this goal.

All the media contain the same basal components, which are DMEM high glucose with sodium piruvate (15-013-CV; Mediatech, Manassas, VA, USA), 15 % (v/v) FBS (14-501F, Lonza, Allendale, NJ, USA), 4 mM L-glutamine (82007-322, VWR, West Chester, PA, USA), 100 µM MEM non essential amino acids (11140-050, Invitrogen, Carlsbad, CA, USA), 100 U/ml penicillin and 0.1 mg/ml streptomycin (20001, JR Scientific, Woodland, CA, USA).

The basal medium was enough to cause cell contraction in the USA because FBS of US origin had the proper growth factors to stimulate the morphogenetic process. Non-US laboratories using European FBS from Sigma (F7524) need to add 0,67 nM PDGF-BB (Sigma, P4056) and 0.02 nM TGF-β (Sigma, T5050) to supplement the FBS of the media. The concentration of PDGF-BB and TGF-β can vary when using different batches of FBS or different commercially available sera. The concentration of these two growth factors was determined by culturing fibroblasts in RAD16-I with different concentrations of PDGF-BB (0.0067 nM, 0.067 nM and 0.67 nM) and TGF-β ($4 \cdot 10^{-4}$ nM, $4 \cdot 10^{-3}$ nM, $2 \cdot 10^{-2}$ nM, $4 \cdot 10^{-2}$ nM and 0.4 nM). IGF-I (Lonza, CC-3162) and VEGF (Lonza, CC-3162) were also used to supplement the medium but they had no significant effect on the contraction of MEFs.

TGF-β was used at different time frames to evaluate the effect of TGF-β along time. We cultured MEFs in medium supplemented with TGF-β 0.02 nM 1) Only the first 3 days. 2) Only the first 5 days. 3) After the first 3 days. 4) After the first 5 days. 5) During all the cell culture. MEFs cultures in the same medium without TGF-β were used as negative controls. The best results were obtained when TGF-β was used during all the morphogenetic process, although there was no significant difference between all these TGF-β supplementation profiles.

3.4.3.3. 3D-Culture with agarose

For the experiments with agarose, the same cells were suspended in FM containing FBS of USA origin. This cell suspension was mixed with an equal volume of 0.5 % Omnipur® agarose (EM Science, Gibbstown, NJ, USA) in 10 % sucrose (S0389, Sigma-Aldrich, St Louis, MO, USA) to obtain a final cell density of $2 \cdot 10^6$ cells/ml in 0.25 % agarose. The cell suspension was briefly cooled until the agarose rendered the gels, which were then equilibrated in FM and incubated as said above.

3.4.3.4. 3D-Culture with Collagen-I

For the experiments with collagen-I, the same cells were suspended in FM containing FBS of USA origin. Isotonic Collagen 0.4 % was prepared diluting commercial Collagen-I (354236 BD, Franklin Lakes, NJ, USA) with filtered 10X PBS (14040, Invitrogen, Carlsbad, CA, USA) and sterile water (Mediatech, Manassas, VA, USA). This solution was neutralized with sterile 1 M NaOH (Sigma-Aldrich, St Louis, MO, USA) using phenol red (P4633, Sigma-Aldrich, St Louis, MO, USA) as indicator. Right after neutralization, equal volumes of the freshly prepared collagen solution and the cell suspension were mixed, to obtain a final cell density of $2 \cdot 10^6$ cells/ml in 0.2 % collagen, and poured inside cell culture inserts. The suspension was heated at 37 ºC so that collagen fibers form a gel inside the inserts. Gels were cultured in FM and incubated as said above.

3.4.4. Differentiation assays

MEFs were cultured in the 3D hydrogels with FM for 12 days and, after that, medium was changed to differentiation medium. MEFs were maintained in differentiation medium for 21 days. As Controls, MEFs were cultured for 33 days in regular fibroblast medium. For osteogenic differentiation, the medium was DMEM high glucose with 10 % FBS, 1 % (v/v) Penicillin streptomycin, 4 mM L-Glutamine and supplemented with Lonza's osteogenic factors: 0.05 mM ascorbate, 10 mM β-glycerophosphate, 0.1 µM dexamethasone and 20 nM 1α,25-$(OH)_2$ vitamin D3 (PT-3002, Lonza, Allendale, NJ, USA).

The medium to induce chondrogenic differentiation was provided by Cambrex (Charles City, IA, USA) and contained Basal Medium supplemented with R^3-IGF, TGF-β, Insulin, Transferrin, FBS and Gentamycin/Amphotericin. The concentrations of all the supplements are not available from the manufacturer.

For the adipogenic differentiation, the medium was DMEM with 10% FBS, 8 µg/ml biotin, 4 µg/ml pantothenate (C8731, Sigma-Aldrich, St Louis, MO, USA), 0.5 mM 3-isobutyl-1-methylxanthine (I7018, Sigma-Aldrich, St Louis, MO, USA), 1 µM dexamethasone (PT-3002, Lonza, Allendale, NJ, USA) and 10 µg/ml insulin (CC-4182, Lonza, Allendale, NJ, USA).

3.4.5. Phenotype assignment

To assign osteoblastic, chondrogenic or adipogenic phenotypes we performed stainings for specific elements of each phenotype. MEFs underwent the previously described differentiation protocols and were stained for calcium deposition (Von Kossa), for Glycosaminoglycan synthesis (Toluidine blue), and for lipidic accumulation (Nile Red) to assess osteogenic, chondrogenic and adipogenic commitments respectively. Stainings were performed as previously described [45, 56, 91].

3.4.6. Western blot analysis

MEFs cultured in different conditions were subjected to lysis in RIPA buffer (BP-115D, Boston Bioproducts, Worcester, MA, USA) containing protease inhibitors (Complete-Mini, Roche, Indianapolis, IN, USA). 2D cultured MEF lysates were used as control protein samples in osteogenic differentiation assays. Cell lysates from these cultures were subjected to NuPAGE® (NP0321, Invitrogen, Carlsbad, CA, USA), transferred onto a PVDF membrane (Invitrolon®, Invitrogen, Carlsbad, CA, USA) and blocked using TBS/Tween with 5 % dry milk. PEBP2αA, Collagen type II was blotted with the indicated antibodies. Actin was used as internal protein standard.

3.4.7. Glycosaminoglycan quantification

GAGs were quantified using DMMB (1,9-dimethyl-dimethyleneblue, 23481-50-7, Polysciences, Warrington, PA, USA). The samples were treated overnight with Pronase at 60 ºC and centrifuged at 14000 g. The supernatant (40 μl) was incubated with 360 μl of a solution of DMMB (0.16% DMMB in 0.2% formic acid [251364, Sigma-Aldrich, St Louis, MO, USA] with 2.5 mg/ml sodium formate [71541, Sigma-Aldrich, St Louis, MO, USA]; pH 3.5) and read in a spectrophotometer with visible light (λ= 535 nm) [92]. Standards of chondroitin 6-sulfate from shark cartilage (27043, Sigma-Aldrich, St Louis, MO, USA) were used to prepare a calibration curve with values between 0 and 100 μg/ml.

3.4.8. Immunostaining of MEFs cultured in RAD16-I

MEFs cultured in RAD16-I during 7 up to 15 days with FM were fixed and washed twice with PBS 1X prepared from 10X PBS (EM-6508, VWR, West Chester, PA, USA). Endogenous peroxidase activity was blocked with 0.3 % hydrogen peroxide in PBST at room temperature for 30 minutes. Samples were blocked with 20 % (v/v) FBS in PBS with 0.1 % (v/v) Triton X-100 (T-9284, Sigma-Aldrich, St Louis, MO, USA) and 1 % (v/v) DMSO (O81-1, Honeywell Burdick and Jackson, Morristown, NJ, USA). Incubation with the indicated primary antibodies was performed overnight at 4 °C. After a 24-hour washing step, samples were incubated overnight at 4 °C with the secondary antibodies-HRP conjugated. Localization of proteins was finally revealed by reaction with DAB substrate (1718906, Roche, Indianapolis, IN, USA).

3.4.9. Cell Cycle Arrest Assays with Staurosporine

Cultures of MEFs were incubated in FM with 20 nM Staurosporine (569397, Calbiochem, Gibbstown, NJ, USA) during 7 days while controls were incubated in FM. At day 6, a pulse of BrdU was applied overnight (16 h). MEFs were fixed at day 7 and stained with a mouse monoclonal antibody IGg1 anti-BrdU FITC-conjugated (BD, Franklin Lakes, NJ, USA). To assess the dose-response effect of staurosporine on MEFs, these were incubated with different concentrations of staurosporine (0, 2, 20 nM) during 14 days. Visual inspection of the cell mass contraction along these 14 days was performed.

3.4.10. Real-time RT-PCR

Reactions using an Applied Biosystems 7900 HT Fast Real-Time PCR Thermocycler

mRNA was isolated with Trizol (15596-026, Invitrogen, Carlsbad, CA, USA) from MEFs, cultured in RAD16-I and cultured in 2 dimensions (controls), at days 3, 7, 11 and 15. After degradation of cellular DNA, first stranded cDNA was synthesized from the mRNA using Taqman Reverse Transcriptase (N808-0234, Applied Biosystems, Foster City, CA, USA). Real-time RT-PCR reactions were performed in SYBR green PCR master mix (204143, Qiagen, Valencia, CA, USA) using commercial primers of Sox9, Runx2, Col2a1, Col1a1 and Col1a2. Relative gene fold variations were all determined by the $2^{-\Delta\Delta Ct}$ Method using the ribosomal unit *18S* (Qiagen) as housekeeping gene.

Reactions using a Corbett Rotor-Gene 3000 thermocycler

mRNA was isolated and purified using an Ambion RNA extraction kit (RNAqueous 4PCR, AM1914). The quantity and purity of this RNA was determined by the absorbance of a diluted (1:50) sample of the extract at λ = 260, 280 and 230 nm. RNA was further used for Real Time PCR only when A_{260} / A_{280} and A_{260} / A_{230} ratios where both between 2 and 2.2; Real Time PCR was performed one-step using SYBR Green as fluorescent reporter (Applied Biosystems, Power SYBR RNA-to-Ct, 4389986). Each reaction was set with a non-template control. All the primers used are listed below. The sequence for the primers of Link Protein was obtained from the literature [93] and the suppliers provided the sequence of the 18S, Sox5 and Sox6 primers.

Relative gene fold variations were all determined by the $2^{-\Delta\Delta Ct}$ Method using the ribosomal unit *18S* (Invitrogen) as housekeeping gene. Gene expression levels in MEFs cultured in culture flasks (2D cultures) were used as reference gene expression levels for the $-\Delta\Delta Ct$ method.

Gene	Supplier	Sequence 5' to 3'
18S	Qiagen	Not available. Quantitect QT01036875
18S	Invitrogen	FW: TTGGAGGGCAAGTCTCGTG RV: CCGCTCCCAAGATCCAACTA
Link Protein	Invitrogen	FW: TGCAGTACCCAATCACCAAACC RV: CTTGTCCCAAAACCCGTAGTTCC
Sox9	Qiagen	Not available. Quantitect QT00163765
Runx2	Qiagen	Not available. Quantitect QT00102193
Col1a1	Qiagen	Not available. Quantitect QT00162204
Col1a2	Qiagen	Not available. Quantitect QT01055572
Col2a1	Qiagen	Not available. Quantitect QT01055523
Sox 5	Qiagen	Not available. Quantitect QT00106218
Sox 6	Qiagen	Not available. Quantitect QT00170891

Figure 12: Primers used for quantitative Real-Time PCR analysis

3.4.11. RT-PCR

mRNA was isolated with Trizol (15596-026, Invitrogen, Carlsbad, CA, USA) from MEFs, cultured in RAD16-I and cultured in 2 dimensions (controls), at days 3, 7, 11 and 15. After degradation of cellular DNA, 0.2 μg of mRNA were retrotranscribed with Omniscript® (205111, Qiagen, Valencia, CA, USA). The cDNA obtained was amplified by PCR (95 °C 2 min, 35 cycles of 95 °C 20 s, 58 °C 30 s and 68 °C 30 s) using Accuprime Pfx (12344-024, Invitrogen, Carlsbad, CA, USA). The primers were kindly provided by Dr David Shaywitz, Harvard University (forward: 5'-CATGTACTCTTTCTTGCTGG-3'; reverse: 5'-GGTCTCGGGAAAGCAGTGGC-3').

3.4.12. Brachyury In situ hybridization

MEF cultures in RAD16-I were fixed at days 7, 11 and 15. *In situ* hybridization was performed whole mount and onto 14 µm slices of the tissue-like cell mass obtained after culturing. Slices were obtained by cryosectioning of the cell-mass with Leica CM 3050 S cryostat using OCT compound (Tissue-tek®, VWR, West Chester, PA, USA) as freezing support. The DNA probe used for the *in situ* hybridization was synthesized with the PCR DIG Probe synthesis kit (11636090910, Roche, Indianapolis, IN, USA) using primers kindly provided by D. Shaywitz (forward primer: CATGTACTCTTTCTTGCTGG; reverse primer: GGTCTCGGGAAAGCAGTGGC). The *in situ* hybridization was performed following the company's instructions for embryos and for tissue sections. After hybridization of the DIG labeled probe, samples were immunostained for digoxigenin using anti-DIG sheep antibody and anti-sheep HRP-conjugated antibody. Reaction with DAB substrate (1718906, Roche, Indianapolis, IN, USA) showed the localization of Brachyury mRNA.

4. The effect of self-assembling peptide nanofiber scaffolds on mouse embryonic fibroblast implantation and proliferation

4.1. *Introduction*

The development of regenerating tissues such as the system described in the previous chapter is a very challenging issue, but is still very far from the bedside. As explained before, the use of materials, cells or combinations of both are much more implanted in the health care system. Beginning in 1950s, surgeons have been using a wide variety of materials for medical applications [94]. Many researchers have developed scaffolds that attempt to mimic natural cell environments in combination with suitable cell types for tissue regeneration. To date, a vast spectrum of biomaterials has been developed using polysaccharides, polypeptides, proteoglycans, lipids, ceramics, biopolymers, as well as complex extracellular matrix components, also in combination with the above [94].

Since in most of the tissues cells are in three-dimensional (3D) environments subjected to special biophysical and biomechanical conditions it is likely that scaffolds mimicking the natural milieu would enhance cell growth and differentiation and therefore they could be a better choice for biomedical applications. For instance, it has already been noted before that calcium phosphates have attracted much attention as biomaterials within the past 20 years due to their ability to facilitate interfacial bonding with bone. In particular, crystalline and semi-crystalline hydroxyapatites (HA) have been recognized as a good bone substitute candidates due to their chemical similarity with naturally calcified tissues, good bioactivity and osteoconductivity [95-99]. Self-assembly of collagen I molecules generates the dermal matrix-equivalent, a soft natural scaffold with pore sizes in the range of 50–200 nm [100]. As said before, engineering of biomimetic materials for soft tissue regeneration are taking advantage of self-assembling peptides with similar mechanical behavior to those of natural collagen scaffolds [101-103] and has provided commercially available synthetic self-assembling peptides for tissue culture. In chapter 3 we have already presented RAD16-I [10] as one of such materials. Briefly, RAD16-I is a AcN-$(RADA)_4$-$CONH_2$ peptide that self-assembles to form a three-dimensional hydrogel structure mimicking the natural extracellular matrix. This biomimetic scaffold has also shown to be non-toxic in vivo and to promote the regeneration of bone tissue in calvarial bone defects [11, 104]. However, an important drawback of RAD16-I is its tendency to break under mechanical stress. In order to improve the mechanical strength of RAD16-I, we have used a composite material consisting of RAD16-I and a previously described porous biorubber scaffold [105]. Biorubbers are elastomeric, rubber-like polymers, with additional biocompatible features [106]. The distinctive characteristic of the proposed composite material is a three-dimensional RAD16-I nanofiber scaffold environment for cells supported in a microporous biorubber scaffold that provides mechanical strength.

Bioluminescence imaging (BLI) procedures [107, 108], based on the detection of visible light photons generated by luciferase reporters expressed by implanted cells, provide an excellent method to asses the viability of cell-scaffold combinations [109, 110]. Photinus pyralis luciferase (PLuc) catalyzes the oxidation of luciferin in the presence of ATP and coenzyme A,

producing light and CO_2. Due to an almost total absence of competing luminescent reactions in mammalian tissues [111], the existence of highly sensitive light measuring instruments and the lack of requirement for post-translational modifications, PLuc is a very convenient and quantifiable cell reporter.

In this chapter we use BLI to study the proliferation behavior of PLuc expressing mouse embryonic fibroblasts, seeded on RAD16-I hydrogels and RAD16-I/biorubber composites to assess the biocompatibility of these scaffold materials. This experimental set-up will allow us to verify if our regeneration model of fibroblasts combined with RAD16-I is applicable *in vivo*.

4.2. *Results*

4.2.1. Mechanical and structural characteristics of the scaffold materials

Shear stress analysis of RAD16-I hydrogels (**Figure 13 A**) showed that the material retains its structure up to a shear stress value of 9 Pa after which shear rate increases dramatically, a typical behavior of non-cross-linked hydrogels. In order to protect the structural integrity of the RAD16-I hydrogel against mechanical deformation, we generated a porous RAD16-I/biorubber composite that would combine the cell growth characteristics of RAD16-I and the mechanical resilience of elastomers. Analysis of the degree of deformation under stress–strain conditions (**Figure 13 B**) showed that both, biorubber and RAD16-I/biorubber behave as typical elastomers, with the presence of RAD16-I resulting in a small reduction of elastic modulus and compression strength, likely due to the plasticizer effect of RAD16-I. The compressive strength of the composite is considerably higher (25,000 Pa) than that of RAD16-I alone (9 Pa). Further creep analysis showed compression deformation behavior also characteristic of elastomeric materials (**Figure 13 C**), having the RAD16-I/biorubber a slightly reduced resistance to deformation.

Structural characterization of the biorubber material by SEM showed (**Figure 16 E,F**) a reasonably uniform 100–150 μm pore size distribution within the range size of cells, but weak pore connectivity.

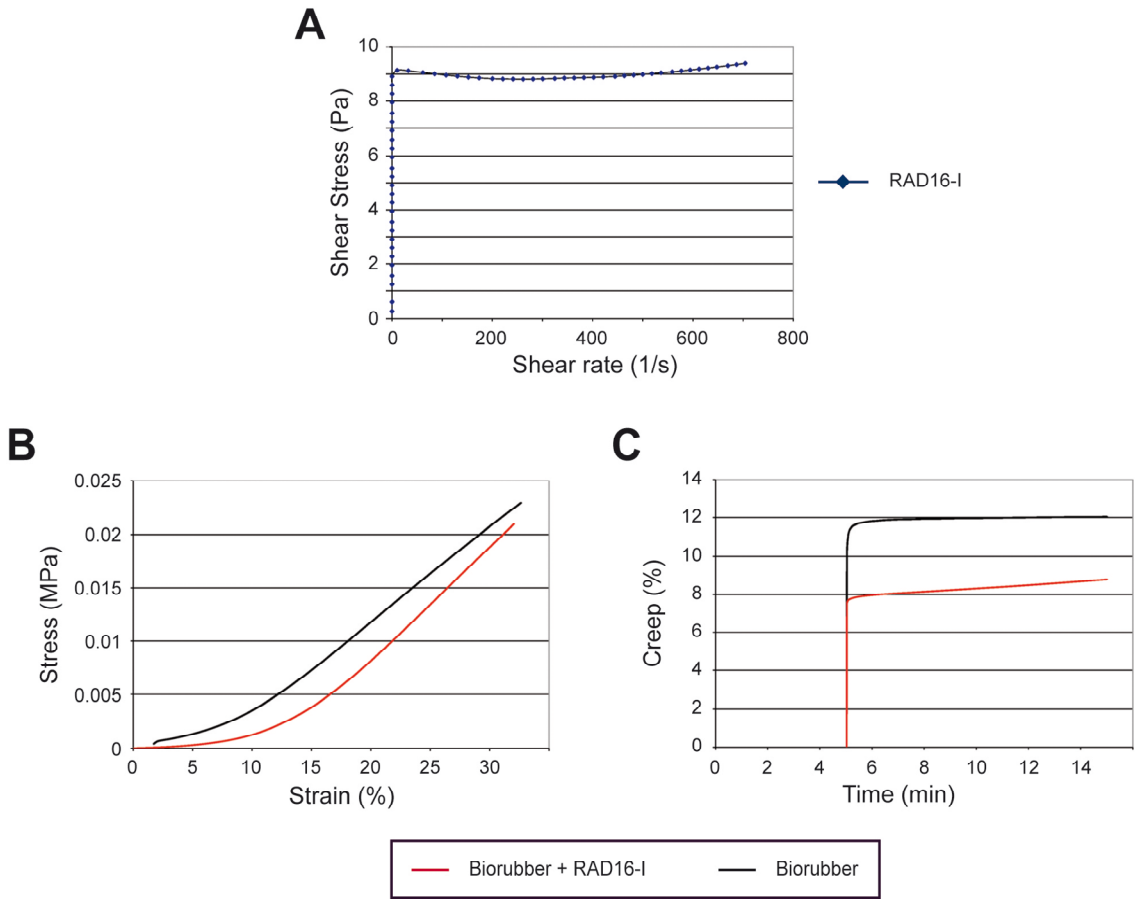

Figure 13: Mechanical properties of RAD16-I and RAD16-I/biorubber.
(**A**) Rheometric curve, shear stress vs. shear rate, of RAD16-I hydrogel. (**B**) Compression stress vs. compression strain (absolute value) for biorubber and RAD16-I/biorubber composite. (**C**) Creep behaviour at compression for biorubber and RAD16-I/biorubber composite.

4.2.2. Light production capacity and stability of G·Luc-C57BL/6 cells in vitro

The amount of light generated by the G·Luc-C57BL/6 cells *in vitro* was determined by measuring the luciferase activity in lysates from predetermined numbers of cells. A standard plot of light production, expressed as relative light units (RLUs) vs. the number of cells in the lysates was generated (**Figure 14 A**) The number of RLUs produced by a single cell is the slope of the linear regression plot, 7.6 RLUs/cell (R^2 = 0.983). Luciferase activity was also measured in cell lysates from in vitro cultures collected every 15 days until the end of the experiment (3 months) to determine the stability of luciferase expression. It was shown that light production capacity, expressed as the RLUs/ng DNA vs. cultivation time, was stable during the 3 months tested (**Figure 14 B**).

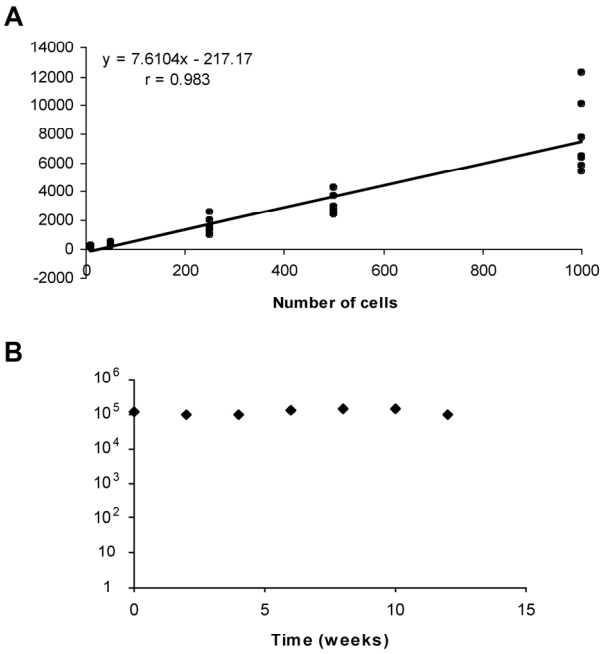

Figure 14: In vitro light production by G·Luc-C57BL/6 cells.
(**A**) Luminometric measurement of luciferase activity (light production) by lysates from 10, 50, 250, 500 and 1000 G·Luc-C57BL/6 cells. Light production is expressed as relative light units (RLUs). The slope of the regression plot (RLUs vs. cell number) is the number of RLUs/cell. (**B**) Stability of luciferase (Luc) expression in vitro. Samples of G·Luc-C57BL/6 cells were collected from a continuous culture every 2 weeks during a 12-week period and analyzed for Luc activity and DNA contents. RLUs/ng DNA is expressed in logarithmic scale.
r = correlation coefficient.

4.2.3. Detection sensitivity for G·Luc-C57BL/6 cells in vivo

To correlate the number of cells with the number of PHCs detected in vivo, predetermined numbers of G·Luc-C57BL/6 cells were inoculated IM in the thighs of nude mice and imaged as previously described. Recorded PHCs were extracted from the images using the Wasabi Software and plotted vs. the number of inoculated cells. The images show that a minimum of 103 G·Luc-C57BL/6 cells could be detected using the high-efficiency ORCA-2BT Imaging System. Moreover, there was a highly linear relationship between cell number and PHCs (R^2 = 0.9873) with a slope of 24.8 PHCs/cell (**Figure 15**). Thus it is possible to correlate PLuc activity with the number of G·Luc-C57BL/6 cells in the implants.

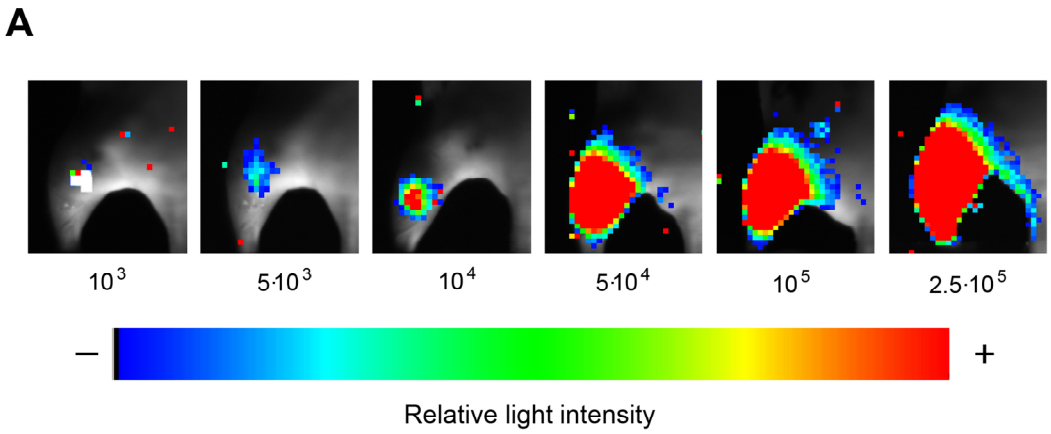

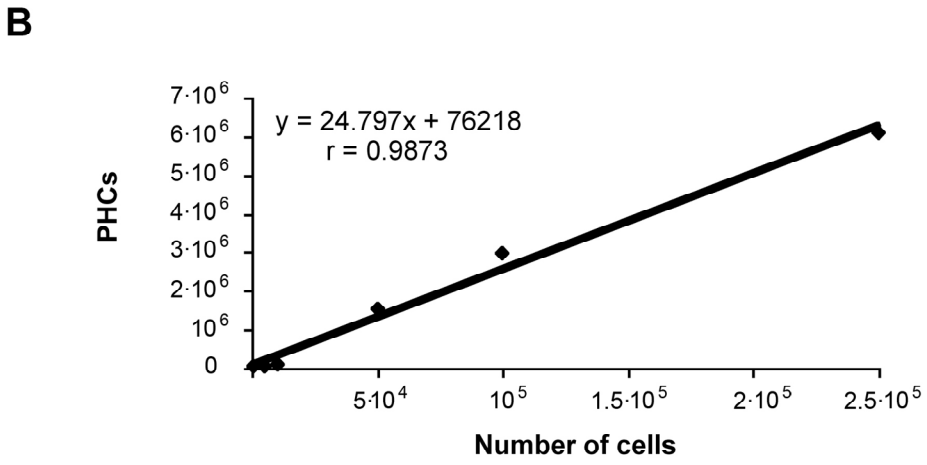

Figure 15: *In vivo* detection of G·Luc-C57BL/6 cells.
(**A**) BLI images of predetermined numbers of G·Luc-C57BL/6 cells (10^3, $5{\cdot}10^3$, 10^4, $5{\cdot}10^4$, 10^5, $2.5{\cdot}10^5$) inoculated intramuscularly in the thighs of nude mice. Pseudo-colour images represent light intensity levels superimposed on white light images of the mice. Arbitrary colour bar: lowest intensity = blue, highest intensity = red. (**B**) Standard plot of photon counts (PHCs) recorded in the images plotted, after background subtraction, vs. the number of inoculated cells. The slope of the regression plot is the number of PHCs/cell, r = correlation coefficient.

4.2.4. In vitro growth of G·Luc-C57BL/6 cells seeded in a RAD16-I hydrogel and RAD16-I/biorubber composite

Cell seeded RAD16-I and RAD16-I/biorubber composites maintained their structure during the three months in vitro. The distribution of cells within the two scaffold materials was evidenced by hematoxylin–eosin staining of histology sections (10 μm thick). **Figure 16 A–D** shows that, while G·Luc-C57BL/6 cells seeded in the RAD16-I hydrogel retained a round morphology and grew forming clusters within the biomaterial (**Figure 16 C**), the same cells seeded in the RAD16-I/biorubber composite neither penetrated into the biorubber nor attached to the material surface, but colonized only the RAD16-I hydrogel structure (**Figure 16 A, B**). Thus, the biorubber appeared to play an exclusively structural role. G·Luc-C57BL/6